2024 IEEE/RSJ International Conference on Intelligent Robots and Systems (IROS)
October 14-18, 2024. Abu Dhabi, UAE

Autonomous Power Line Tracking with mmWave Radar

Nicolaj Haarhøj Malle[1], Emad Ebeid[1]

***Abstract*— This work proposes a novel drone system designed to autonomously track and follow power lines and reconstruct them in 3D with a point cloud representation based on mmWave radar measurements. The system is composed of a GNSS-enabled quadrotor UAV equipped with a combined mmWave radar sensor and onboard compute module payload and has been designed to be small, lightweight, and low-cost. MmWave radar sensors offer great range and sensitivity in the task of power line detection with a high level of sparsity in the produced data when compared to traditional sensors such as LiDARs. The proposed system overcomes the radar sensor's shortcomings by building up a point cloud representing the power line environment as the drone moves around in it. The built-up point cloud is analyzed using the onboard computer to detect the cables in the power line environment and to produce pose-estimates of each line. The system has been tested in a variety of scenarios and has been shown to be able to accurately detect and track power lines in varying weather conditions.**

A video demonstration of the system can be viewed here: https://www.youtube.com/watch?v=MORFX3CFygk.

I. Introduction

Many countries are experiencing rising electrification of their societies which increases the reliance on well-functioning power grids. To monitor the health of this critical infrastructure and minimize its downtime, grid operators must constantly inspect their assets. Traditionally, such inspections are performed manually using helicopters or cranes. However, with the advent of small Unmanned Aerial Vehicles (UAVs), smarter solutions are being researched [1] [2] [3]. Currently, most commercial UAV-based infrastructure inspection is still manually piloted or deployed as simple pre-programmed waypoint missions. However, fully autonomous inspection systems, paired with self-recharging technology [4], would be significantly more valuable to grid operators. Autonomous systems presented in recent research [5] [6] [7] [8] typically rely on optical sensors such as LiDARs to detect and track the infrastructure. These sensors may suffer from reduced performance in fog, as seen in Fig. 1, smog, smoke, and precipitation [9] [10] [11].

As shown in [12] [13] [14], Frequency-Modulated Continuous Wave (FMCW) mmWave radar offers significant advantages over many other sensor technologies in the domain of power line perception. These sensors operate at frequencies between 24 and 81 GHz where many materials become partly transparent, while metallic objects remain highly reflective. This is advantageous when the main objects of interest, such as power lines and transmission towers, mostly consist of steel and aluminum. The result is a sensor that is able to detect power lines at distances approaching 40 m [15] even in poor weather conditions. In addition, mmWave radar sensors are lightweight (<50 g), cost-effective (<200 USD), energy efficient (<3 W), solid-state, and about the size of a credit card. Finally, they produce sparse and high-quality data, which makes them useful in compute-restricted environments such as onboard a UAV.

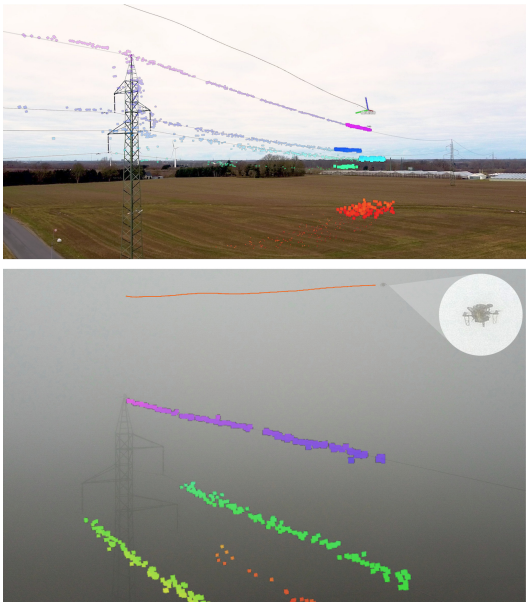

Fig. 1: Autonomous UAV at the start of a cable following mission on a clear day and in heavy fog with visualizations of its path and generated reconstruction used for path planning.

This work addresses some of the shortcomings perceived in the current literature on autonomous power line tracking UAVs by leveraging the advantages of mmWave radar. The presented system is a UAV-based power line inspection platform that offers superior performance in adverse weather conditions. It autonomously tracks power line cables at desired velocities while maintaining a configurable distance to them. High-speed power line tracking can be achieved because the system is not affected by motion blur. An internal 3D reconstruction of the power lines enables robust, programmable cable tracking. Overall, the system is highly configurable with more than 30 adjustable parameters that affect distance, speed, which power line to track, throughput of the perception system, etc. These capabilities ease infras-

This work was supported by the European Union's Horizon 2020 Research and Innovation Programme under grant agreement No. 861111 (Drones4Safety) and the European Union's Horizon 2020 Research and Innovation Programme under grant agreement No. 871479 (AERIAL-CORE). Special thanks to G. Cioffi, C. Pfeiffer, and D. Scaramuzza at the Robotics and Perception Group, University of Zurich.

[1] The authors are with Drone Infrastructure Inspection and Interaction Group, University of Southern Denmark, email: nhma@sdu.dk

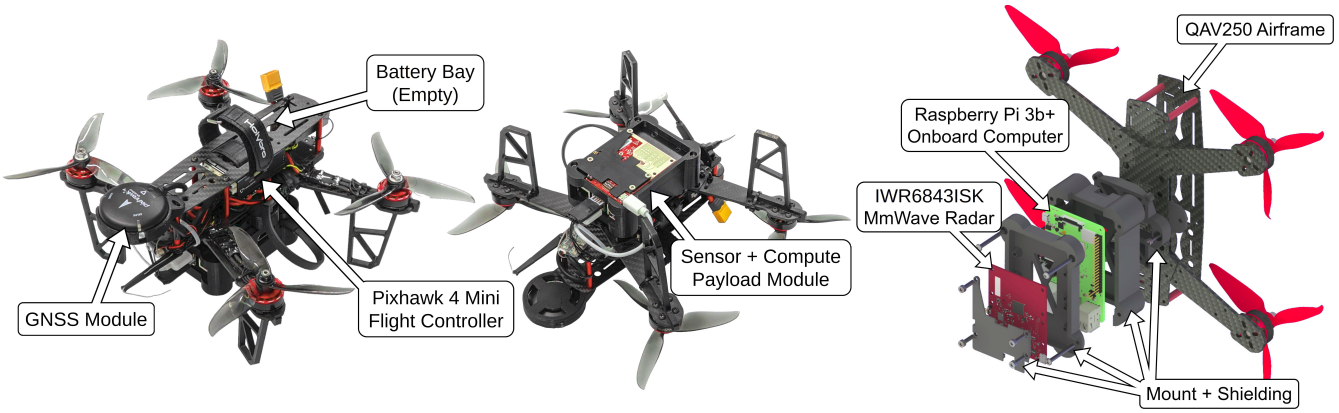

Fig. 2: The sensor and compute module mounted to the underside of a Holybro QAV250 airframe.

tructure inspection and mapping tasks by allowing the system to operate autonomously without the need for a skilled pilot.

The main contributions of this work are:

- Configurable, autonomous power line tracking using low-cost mmWave radar for increased weather and lighting robustness;
- 3D point cloud reconstruction of power transmission lines and towers for navigation from sparse radar data;
- Validation in high-voltage transmission power line and railway environments;
- Extensive flight testing under different weather conditions.

The remainder of the paper is structured as follows: Sec. II summarizes related work; Sec. III describes the hardware setup; Sec. IV explains the processing of sensor data to obtain the power line reconstructions; Sec. V describes the experiments performed to validate the system; and Sec. VI concludes on the findings of the work.

II. Related Work

We have previously shown how FMCW mmWave radar sensors can be used to perform power line detection [12] [13] [14]. However, these systems utilize additional sensors in conjunction with the radar sensor and function in a fundamentally different way to enable delicate near-cable maneuvers rather than cable tracking and tower crossing.

Most power line detection methods in literature are based on processing of RGB images, both using classical computer vision such as PLineD [16] or with deep learning implementations such as presented by Madaan et al. [17] and Son et al. [18]. Zhou et al. [8] demonstrate a vision-based autonomous power line following system, and Wang et al. [19] [20] present a system similar to other vision-based systems but with the addition of radar for one-dimensional distance measurement to the power lines. Less frequently explored methods for power line detection includes the use of event cameras, as shown by Dietsche et al. [21], and magnetic field analysis, as presented by Moore et al. [22]. These systems either produce rudimentary or no information on the distance to the power line, and none of them result in a reconstruction.

In the literature, power line reconstruction is usually achieved by utilizing laser scanning devices or with photogrammetric methods. Pastucha et al. [23] show how images captured from a UAV can be used to reconstruct the power line corridor. However, photogrammetric algorithms are typically run offline. Other approaches for reconstructing power line corridors in 3D typically utilize laser scanning strategies, such as presented by Guo et al. [24] and Azevedo et al. [25]. Lidars typically incur a significant cost and putting one on a UAV comes with a weight penalty and the risk of crashing with expensive equipment.

III. Hardware Setup

The QAV250 airframe offers in excess of 1kg takeoff weight while keeping physical dimensions constrained. The Pixhawk 4 Mini flight controller runs the PX4 [26] v1.13.0 software stack built from source with Real-Time Publish Subscribe (RTPS) support. The sensor and compute payload module, of which an exploded view can be seen in Fig. 2, consists of a Texas Instruments IWR6843ISK [27] FMCW mmWave radar sensor for perception connected via USB to a Raspberry Pi 3b+ [28] which handles the onboard computations related to perception and autonomous flight. The Raspberry Pi has 1 GB of LPDDR2 SRAM available and runs Ubuntu [29] with ROS2 [30] as the middle-ware. The radar sensor is flashed with the out-of-box firmware and configured to operate in 3D mode (3RX, 4TX) with a data rate of 25 Hz. The field of view of the radar sensor is approximately 120° azimuth and 40° elevation. A custom protective housing holds the Raspberry Pi and radar together and mounts the whole package to the underside of the airframe such that the radar sensor faces downwards. Tab. I presents the price, weight, and size of the parts comprising the system. A battery is not listed as this may vary.

TABLE I: Bill of materials of drone platform components.

Name	Price (US$)	Weight (g)	Size (mm)
Holybro QAV250 (Incl. GPS & flight controller)	288	400	85x276x327
Raspberry Pi 3b+	49	50	26x85x54
TI IWR6843ISK radar	175	40	27x96x8
Cables, 3D prints	20	135	-
Total	522	625	183x276x327

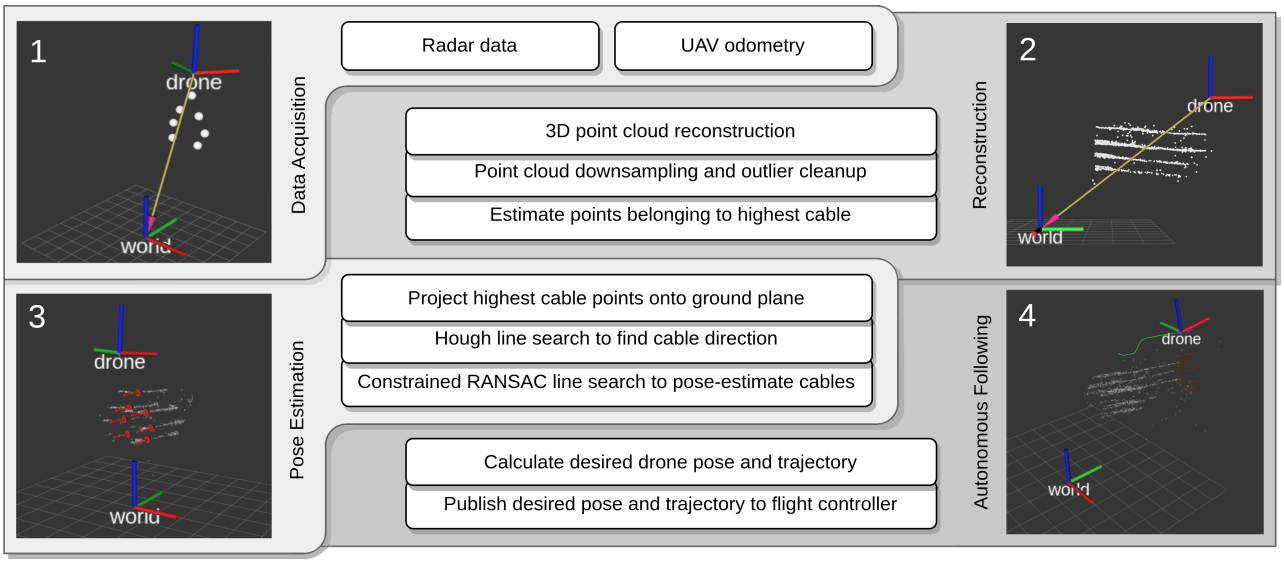

Fig. 3: The four different main stages of the onboard computations and their outputs; Radar and odometry data acquisition, point cloud reconstruction, individual cable pose estimation, and autonomous power line tracking.

IV. Radar Perception System

The perception system, as outlined in Fig. 3, is based on point cloud data from the radar sensor as well as the estimated state of the drone from the flight controller. The drone state importantly includes the drone's position, orientation, and velocity whereas each new data frame from the radar device typically contains one 3D point per power line within the sensor's field of view. To assess the performance of the radar device on power line reconstruction tasks, data from more than 40 reconstructions has been analyzed to produce Fig. 4. The data indicates that the density of the reconstruction (i.e. how many 3D points are produced by the radar device per meter of power line) decreases linearly from close to the theoretical maximum (6.25 pts/m with 25 Hz radar and 4 m/s velocity) down to 0 when the distance to the power line increases from 10 to 30 meters. Similarly, the average distance between individual points and

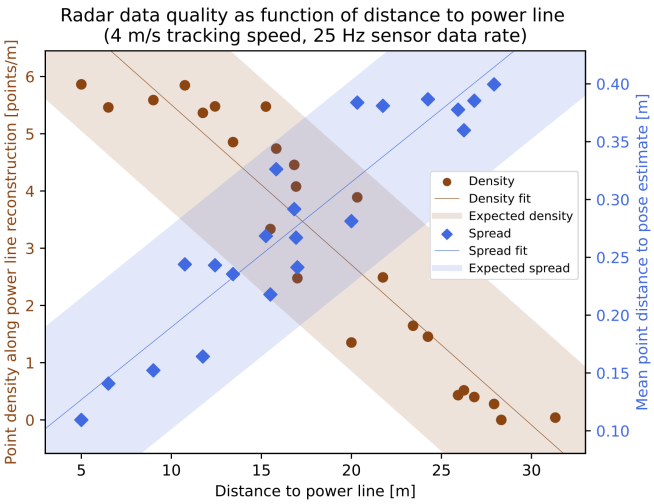

Fig. 4: Distance between the sensor and power line affects the number of measurements and the variance of the data.

the pose estimate of the reconstruction quadruples over the same change in distance to the power line. Fig. 5 shows two reconstructions of the same 20 m segment of a single 10 mm Ø cable after they are projected along the power line direction. The reconstruction produced when the drone was further away (20 m) exhibits significantly more spread perpendicular to the power line axis as well as lower density (only 34 points in reconstruction vs 115) compared to the closer reconstruction (5 m). Based on the data, the maximum usable range of the radar for power line reconstruction is around 25 m. Due to safety concerns, the minimum range evaluated is 4 m.

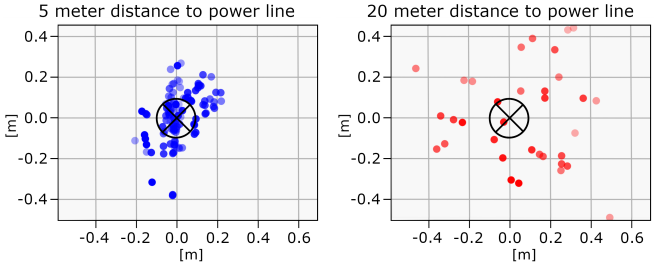

Fig. 5: Example of spread in reconstructions relative to estimated power line pose (⊗) at two different distances.

The overall data flow in the reconstruction and tracking pipeline is shown in Fig. 6. Upon reading a new radar point cloud $\boldsymbol{D}$, individual points ${}^{i}_{l}\boldsymbol{D}$ are filtered based on the expected maximum range r_{max} as well as azimuth θ_r and elevation ϕ_r of the IWR6843ISK radar device to satisfy that

$$\begin{aligned} ||\,{}^{i}_{l}\boldsymbol{D}\,|| &\leq r_{max}, \quad \text{and} \\ \tan^{-1}\left(\frac{{}^{i}_{l}D_y}{{}^{i}_{l}D_x}\right) &\leq \theta_r, \quad \text{and} \\ \tan^{-1}\left(\frac{{}^{i}_{l}D_z}{{}^{i}_{l}D_x}\right) &\leq \phi_r, \quad \forall i = 1,\ldots,l \end{aligned} \tag{1}$$

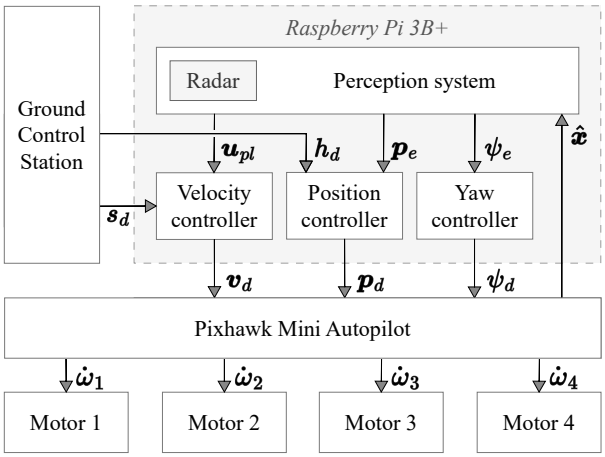

Fig. 6: Autonomous power line tracking data scheme.

This filtering step significantly reduces the occurrence of phantom points, as shown in Fig. 7

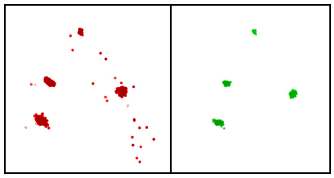

Fig. 7: Four reconstructed power lines projected along the power line direction. **Left**: unfiltered. **Right**: filtered.

Each point is then transformed from the radar frame of reference to the world frame W given the calibrated static transform $\boldsymbol{T}_D^R$ from radar frame R to the drone frame D and the transform $\boldsymbol{T}_W^D$ as derived from the flight controller state estimate $\hat{\boldsymbol{x}}$.

$$\boldsymbol{D}_W = \boldsymbol{T}_D^R \boldsymbol{T}_W^D \boldsymbol{D}_R \tag{2}$$

The transformed point cloud is then concatenated with the existing global point cloud in the world frame $\boldsymbol{G}_W$.

$$\boldsymbol{G}_W = (\boldsymbol{G}_W \mid \boldsymbol{D}_W) \tag{3}$$

A local horizon H is defined as a cube with side length l and center at the current drone position in the world frame $\boldsymbol{p}_W$. Points outside H are discarded to lower computational intensity and preserve local accuracy in the later point cloud operations. This results in a point cloud $\boldsymbol{L}$ where each of its m points satisfies that

$$|| \, {}_m^i\boldsymbol{G}_W - \boldsymbol{p}_W \, || \leq l \qquad \forall i = 1, ..., m \tag{4}$$

Next, the average height $\bar{h}$ of the highest cluster of points in $\boldsymbol{L}$ is found. $\bar{h}$ is used to define the height of the center of a box with lateral side lengths l and vertical side length v where $l > v$ such that the box is relatively flat. All points in $\boldsymbol{L}$ that lie inside this flat box define a new point cloud $\boldsymbol{G}$, similar to Eq. 4. All n points in $\boldsymbol{G}$ are then projected onto the ground plane, defined by the point $\boldsymbol{O}$ and the normal $\boldsymbol{g}$ (negative gravity direction), to create a 2D representation $\boldsymbol{H}$.

$${}_n^i\boldsymbol{H}_W = ({}_n^i\boldsymbol{G}_W - \boldsymbol{O}_W) \cdot \boldsymbol{g}_W \qquad \forall i = 1, ..., n \tag{5}$$

$\boldsymbol{H}$ now only contains points belonging to the cluster with the highest z component. When flying above power lines, this will correspond to measurements of the topmost cable(s). The reasons for focusing on this volume are two-fold: 1) given that it is the closest to the drone, it will have been measured most often and most reliably by the radar, and 2) the top line is typically one or a few widely separated wires. Therefore, when looking at the projected points in $\boldsymbol{H}$, there should be a clear direction visible within the xy-plane. The Hough Line Transform [31] is applied to $\boldsymbol{H}$ to extract this 2D direction $\boldsymbol{c}$ within the xy-plane.

Random sample consensus (RANSAC) is then used to fit 3D sticks $\boldsymbol{s}$ on the points in the local horizon $\boldsymbol{L}$ that satisfy

$$\begin{aligned} \cos^{-1}\left(\frac{\boldsymbol{s} \cdot \boldsymbol{c}}{|| \, \boldsymbol{s} \, || \, || \, \boldsymbol{c} \, ||}\right) \leq t_\psi, \quad \text{and} \\ \tan^{-1}\left(\frac{\sqrt{s_x^2 + s_y^2}}{s_z^2}\right) \leq t_\theta \end{aligned} \tag{6}$$

where t_ψ is the maximum allowed angle between $\boldsymbol{c}$ and $\boldsymbol{s}$, t_θ is the maximum allowed pitch angle of $\boldsymbol{s}$. Introducing t_ψ and t_θ reduces the computational intensity by limiting the RANSAC search space and acts as a parallelism constraint for the resulting pose estimates.

To reduce false positives, e.g. from branches and fences, each fitted stick's point density ρ_s and spread σ_s must be within the expected regions of density ρ_e and spread σ_e for power lines (Fig. 4) given the distance to the power line d_l and current tracking speed v_c.

$$\begin{aligned} | \, (\rho_s - \rho_e(d_l, v_c)) \, | \leq \rho_t, \quad \text{and} \\ | \, (\sigma_s - \sigma_e(d_l, v_c)) \, | \leq \sigma_t \end{aligned} \tag{7}$$

where ρ_t and σ_t are the thresholds for the expected density and spread regions, respectively.

Each valid stick fit is then projected onto the plane defined by the drone position $\boldsymbol{p}_W$ and the average direction of all stick fits, similar to Eq. 5 This yields the powerline pose estimates $\boldsymbol{E}$ on the closest point on each cable relative to $\boldsymbol{p}_W$, as represented by the red arrows in window 3 in Fig. 3. Pose estimates are tracked over time within this plane where they stay alive when new matches are found in consecutive pose estimation operations or otherwise decay over time.

Given the position and yaw errors $\boldsymbol{p}_e$ and ψ_e relative to the targeted powerline pose estimate as well as the target powerline tracking speed s_d, the desired trajectory setpoints can be sent to the Pixhawk flight controller as follows

$$\begin{aligned} \boldsymbol{v}_d = s_d \, {}^k\boldsymbol{E}_d, \quad \text{and} \\ \boldsymbol{p}_d = \boldsymbol{p}_W + (\boldsymbol{p}_W - \boldsymbol{p}_e) k_p, \quad \text{and} \\ \psi_d = \psi_c + (\psi_c - \psi_e) \cdot k_\psi \end{aligned} \tag{8}$$

where ${}^k\boldsymbol{E}_d$ is the direction vector of the targeted power line's pose estimate and k_v, k_p, and k_ψ are empirically tuned proportional gains.

V. Results

Fig. 8 shows the alignment errors during a cable tracking mission covering around 260 m including two tower crossings marked by vertical lines.

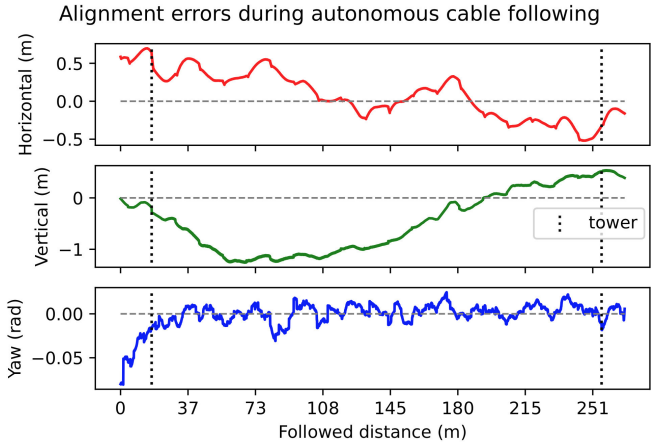

Fig. 8: Alignment errors during cable tracking relative to perceived cable at 5 m/s speed with crosswinds up to 7 m/s.

The target speed was 5 m/s and the target vertical distance to the tracked cable was 5 m. After initial alignment, the yaw error was typically between ± 0.03 radians ($\pm 1.72°$). The peak horizontal error of around 0.5 m is most likely because of the observed crosswind of up to 7 m/s. The peak vertical error at around 1 m and the curve it seems to follow is an artifact of the linear representation of the hyperbolic cosine curvature of the cable within the sliding window perception horizon of the drone. Crossing the transmission towers did not have a significant impact on tracking accuracy.

During both tower crossings, the horizontal distance between the drone's estimated position, as obtained from the flight controller, and a geo-referenced position for the center of each tower was below 20 cm.

Other tests were performed to validate the system's robustness to impaired visual conditions. In one such test the system performed a similar tracking mission in dense fog, showing no apparent impairment and producing similar results as seen in Fig. 8. The conditions of the test with the drone performing autonomous cable tracking can be seen in Fig. 1.

The maximum successfully tested tracking speed is 8 m/s. The increased pitch of the drone at even higher speeds significantly degrades the radar data as the angle between the radar beam and the power line direction becomes less perpendicular, which significantly reduces the number of points produced by the radar. Similarly, the tracking with the largest distance to the target cable is around 20 m for a cable with a diameter of 10 mm. At greater distances, the radar data becomes too sparse to reliably pose estimate the power lines. The relationship between the quality of the radar data and the distance to the power line can be seen in Fig. 4 which suggests a significant negative correlation.

Tab. II compares the test results of the presented system with related systems from the literature. As the table illustrates, the presented system is simultaneously among the cheapest, smallest, and lightest while outperforming most of the related systems on most parameters. By relying on radar rather than LiDAR, the system remains lightweight and inexpensive while still able to produce 3D reconstructions from depth information. High tracking and following speeds are enabled by the high data rate of the radar sensor and fast data processing of the sparse data. This is key when optimizing the use of the limited flight time of a drone, as higher speeds typically result in longer distances covered [33].

Fig. 9 shows data from another autonomous cable tracking mission including a tower crossing. The tracking speed was 5m/s and the distance to the target cable was 7 meters. The two satellite projection images **a** and **b** indicate that the path taken and reconstruction produced align well with the observed real-world structures. The 3D reconstruction in **c** shows the easily distinguishable individual power lines as well as the structure of the tower. Measurements of the ground (shown in orange and red) are ignored during autonomous flight by filtering them based on the UAV's estimated height above ground.

Work / Category	Schofield [5]	Takaya [6]	Cerón [7]	Bian [32]	Zhou [8]	Wang [19]	Ours
Sensors	LiDAR+GNSS	LiDAR+RTK	Cam.+GNSS	Cam.+GNSS	Cam.+GNSS	Cam.+Radar+GNSS	Radar+GNSS
Depth information	**Yes**	**Yes**	No	No	No	**Yes**	**Yes**
3D Reconstruction	No	No	No	No	No	No	**Yes**
Max. following speed	0.5 m/s	1.4 m/s	0.5 m/s	-	**8 m/s**	0.3 m/s	**8 m/s**
Max. power line dist.	6 m	-	-	-	-	2.5 m	**17 m**
Tracking accuracy	**0.3 m**	0.5 m	1 m	-	1-2 m	0.7 m	0.6 m
Weight	1.8 kg	6 kg	0.7 kg	1.8 kg	1 kg	**0.5 kg**	1 kg
Hardware price	1600 $US[a]	10000 $US[a]	600 $US[a]	3000 $US[a]	1000 $US[a]	600 $US[a]	**522 $US**
Wheelbase	60 cm	85 cm	55 cm	65 cm	35 cm	**25 cm**	**25 cm**

[a] Estimates based on sensor, computer, and drone frame prices.

– Information not found.

TABLE II: Comparison between this work and other power line tracking systems found in literature.

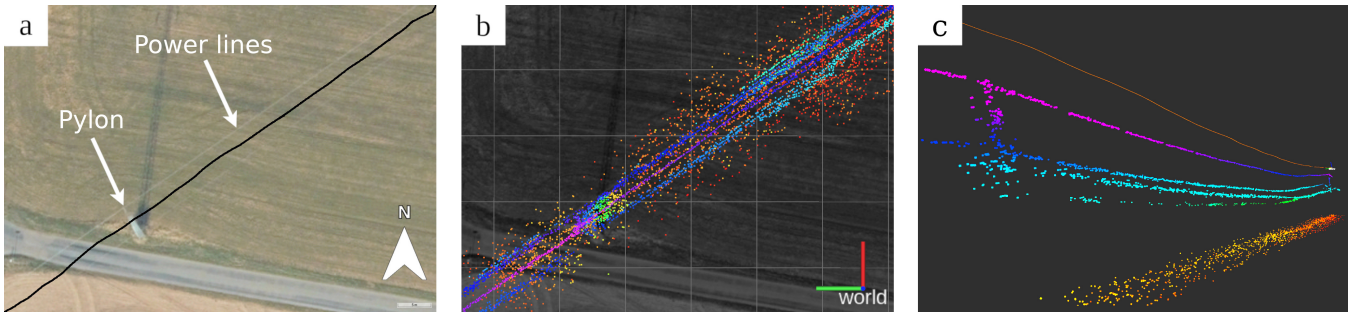

Fig. 9: **a)** Satellite image of a stretch of power lines with UAV autonomous path in black. **b)** Reconstruction projected onto satellite image. **b)** 3D reconstruction with the autonomous flight path in orange.

A. *Railway Inspection Use-Case*

Besides power line tracking, the system has been tested for autonomous railway inspections. Equipped with a downward-facing inspection camera, the system tracks and follows the overhead railway power line in a similar fashion to the transmission power line use-case, while recording images of the track and other infrastructure assets. This setup was tested at the Siemens PCW test facility Wegberg, Germany, where the system autonomously collected data on a segment of railway track. Fig. 10 shows a snapshot of this test, including the inspection camera view in the upper left and the overhead line reconstruction and autonomous path in the lower left. Fig. 11 shows the performance throughout the mission, including adapting to changing power line distance setpoints. Overall, the system is highly configurable and allows user-defined tracking distances and speeds, options to choose which power line to track, throughput of the perception system, filtering strategy, etc. These parameters are useful when deploying the system in a new environment, like moving from transmission lines to railway lines.

This test also highlighted the potential applicability of the system as a pilot assistance tool. Humans perform suboptimally when estimating the distance to power lines [34] [35], and the proposed system has the potential to make manual drone operations near power lines safer. For the railway inspection flights, the pilot's job was to fly the drone above the target line to follow, after which they engaged the onboard autonomy. From here, their task was to monitor the data and adjust the tracking distance and speed as desired without worrying if the drone was in fact above the line at the correct distance.

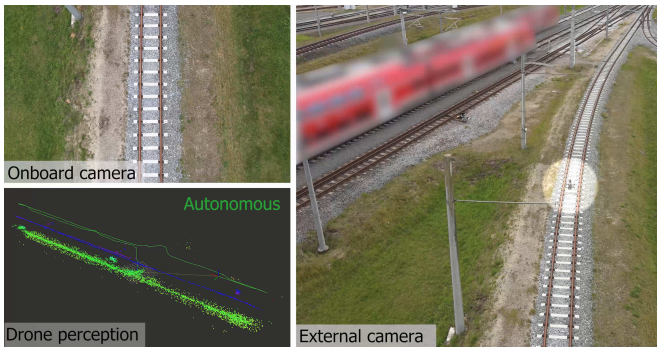

Fig. 10: Railway inspection demonstration at Siemens PCW.

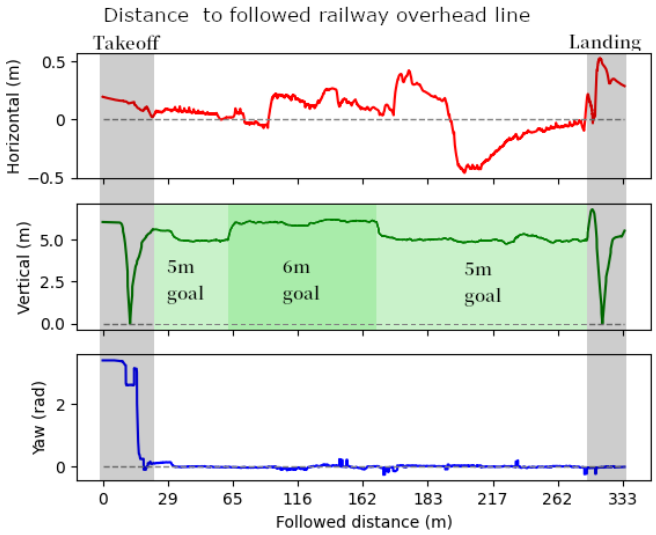

Fig. 11: Results of railway overhead line tracking, including behavior during changing distance setpoint.

VI. Conclusion

This paper presented a drone system for autonomously tracking and following power lines based on onboard radar measurements and computations. The onboard navigation scheme reconstructs the tracked power lines in 3D and pose-estimates each cable to plan a tracking trajectory. Testing shows that the software runs well in a resource-constrained environment and is adjustable to operate with changing requirements. The system was validated in both power line and railway environments in various weather conditions. The use of radar rather than electro-optical sensors allows the system to be agnostic to varying weather and lighting conditions. The system is smaller and cheaper than systems otherwise found in the literature, and results show that it is able to autonomously follow power lines at speeds up to 8 m/s and track cables at maximum distances of 17 m while maintaining a minimal tracking error.

REFERENCES

[1] "IFD Drones4Energy Project." [Online]. Available: https://drones4energy.dk/

[2] "AERIAL COgnitive integrated multi-task Robotic system with Extended operation range and safety." [Online]. Available: https://aerial-core.eu/

[3] "H2020 Drones4Safety Project." [Online]. Available: https://drones4safety.eu/

[4] V. Hoang, F. Nyboe, N. Malle, and E. Ebeid, "Autonomous Overhead Powerline Recharging for Uninterrupted Drone Operations (accepted)." International Conference on Robotics and Automation (ICRA), 2024.

[5] O. B. Schofield, N. Iversen, and E. Ebeid, "Autonomous power line detection and tracking system using uavs," *Microprocessors and Microsystems*, 2022.

[6] K. Takaya, H. Ohta, K. Shibayama, and V. Kroumov, "Tracking Control of Unmanned Aerial Vehicle for Power Line Inspection," in *Motion Planning*, E. A. M. García, Ed. Rijeka: IntechOpen, 2021, ch. 2. [Online]. Available: https://doi.org/10.5772/intechopen.100067

[7] A. Cerón, I. Mondragón, and F. Prieto, "Onboard visual-based navigation system for power line following with uav," *International Journal of Advanced Robotic Systems*, 2018.

[8] G. Zhou, J. Yuan, I.-L. Yen, and F. Bastani, "Robust real-time UAV based power line detection and tracking," in *2016 IEEE International Conference on Image Processing (ICIP)*, 2016, pp. 744–748.

[9] Y. Li, P. Duthon, M. Colomb, and J. Ibanez-Guzman, "What happens for a tof lidar in fog?" *IEEE Transactions on Intelligent Transportation Systems*, 2021.

[10] J. Pascoal, L. Marques, and A. T. de Almeida, "Assessment of laser range finders in risky environments," in *2008 IEEE/RSJ International Conference on Intelligent Robots and Systems*, 2008.

[11] M. Bijelic, T. Gruber, and W. Ritter, "A benchmark for lidar sensors in fog: Is detection breaking down?" in *2018 IEEE Intelligent Vehicles Symposium (IV)*, 2018.

[12] N. H. Malle, F. F. Nyboe, and E. Ebeid, "Survey and Evaluation of Sensors for Overhead Cable Detection using UAVs," in *2021 International Conference on Unmanned Aircraft Systems (ICUAS)*, 2021, pp. 361–370.

[13] F. F. Nyboe, N. H. Malle, G. v. Bögel, L. Cousin, T. Heckel, K. Troidl, A. S. Madsen, and E. Ebeid, "Towards Autonomous UAV Railway DC Line Recharging: Design and Simulation," in *2023 IEEE International Conference on Robotics and Automation (ICRA)*, 2023, pp. 3310–3316.

[14] N. H. Malle, F. F. Nyboe, and E. S. M. Ebeid, "Onboard Powerline Perception System for UAVs Using mmWave Radar and FPGA-Accelerated Vision," *IEEE Access*, vol. 10, pp. 113 543–113 559, 2022.

[15] Barrett, Dennis et al., "Using mmwave sensors to enhance drone safety and productivity," *Texas Instruments white paper SPYY001*, 2017.

[16] T. Santos, M. Moreira, J. Almeida, A. Dias, A. Martins, J. Dinis, J. Formiga, and E. Silva, "Plined: Vision-based power lines detection for unmanned aerial vehicles," in *2017 IEEE International Conference on Autonomous Robot Systems and Competitions (ICARSC)*, 2017, pp. 253–259.

[17] R. Madaan, D. Maturana, and S. Scherer, "Wire detection using synthetic data and dilated convolutional networks for unmanned aerial vehicles," in *2017 IEEE/RSJ International Conference on Intelligent Robots and Systems (IROS)*, 2017, pp. 3487–3494.

[18] H.-S. Son, D.-K. Kim, S.-H. Yang, and Y.-K. Choi, "Real-Time Power Line Detection for Safe Flight of Agricultural Spraying Drones Using Embedded Systems and Deep Learning," *IEEE Access*, 2022.

[19] Q. Wang, W. Wang, Z. Li, A. Namiki, and S. Suzuki, "Close-range transmission line inspection method for low-cost uav: Design and implementation," *Remote Sensing*, 2023.

[20] W. Wang, Z. Shen, and Z. Zhou, "A novel vision- and radar-based line tracking assistance system for drone transmission line inspection," *Remote Sensing*, 2024.

[21] A. Dietsche, G. Cioffi, J. Hidalgo-Carrió, and D. Scaramuzza, "Powerline Tracking with Event Cameras," in *2021 IEEE/RSJ International Conference on Intelligent Robots and Systems (IROS)*, 2021, pp. 6990–6997.

[22] J. Moore and R. Tedrake, "Magnetic localization for perching UAVs on powerlines," in *2011 IEEE/RSJ International Conference on Intelligent Robots and Systems (IROS)*, 2011.

[23] E. Pastucha, E. Puniach, A. Ścisłowicz, P. Ćwiąkała, W. Niewiem, and P. Wiącek, "3D Reconstruction of Power Lines Using UAV Images to Monitor Corridor Clearance," *Remote Sensing*, 2020.

[24] B. Guo, Q. Li, X. Huang, and C. Wang, "An Improved Method for Power-Line Reconstruction from Point Cloud Data," *Remote Sensing*, 2016.

[25] F. Azevedo, A. Dias, J. Almeida, A. Oliveira, A. Ferreira, T. Santos, A. Martins, and E. Silva, "Real-Time LiDAR-based Power Lines Detection for Unmanned Aerial Vehicles," in *International Conference on Autonomous Robot Systems and Competitions (ICARSC)*, 2019.

[26] PX4. "PX4 Autopilot website". Visited on 03/03/2024. [Online]. Available: https://px4.io/

[27] Texas Instruments. "IWR6843ISK product page". Visited on 03/03/2024. [Online]. Available: https://www.ti.com/tool/IWR6843ISK

[28] Raspberry Pi Foundation. "Raspberry Pi 3+ Model B product page". Visited on 03/03/2024. [Online]. Available: https://www.raspberrypi.com/products/raspberry-pi-3-model-b-plus/

[29] Ubuntu. "Install Ubuntu on a Raspberry Pi". Visited on 03/03/2024. [Online]. Available: https://ubuntu.com/download/raspberry-pi

[30] Open Robotics. "Robot Operating System (ROS)". Visited on 03/03/2024. [Online]. Available: https://www.ros.org/

[31] R. O. Duda and P. E. Hart, "Use of the Hough transformation to detect lines and curves in pictures," *Communications of the ACM*, vol. 15, no. 1, p. 11–15, jan 1972. [Online]. Available: https://doi.org/10.1145/361237.361242

[32] J. Bian, X. Hui, X. Zhao, and M. Tan, "A novel monocular-based navigation approach for uav autonomous transmission-line inspection," in *2018 IEEE/RSJ International Conference on Intelligent Robots and Systems (IROS)*, 2018.

[33] L. Bauersfeld and D. Scaramuzza, "Range, endurance, and optimal speed estimates for multicopters," *IEEE Robotics and Automation Letters*, vol. 7, no. 2, pp. 2953–2960, 2022.

[34] R. Q. Brackett, V. J. Pezoldt, and L. Roush, "Estimating the height of a suspended wire," *Proceedings of the Human Factors Society Annual Meeting*, vol. 36, no. 13, pp. 955–959, 1992. [Online]. Available: https://doi.org/10.1177/154193129203601307

[35] D. Imbeau, J.-J. Paques, S. Bergeron, and R. Bourbonnière, "Comparison of two methods for judging distances near overhead power lines," *International Journal of Occupational Safety and Ergonomics*, vol. 2, no. 3, pp. 196–211, 1996, pMID: 10602585. [Online]. Available: https://doi.org/10.1080/10803548.1996.11076348